Time-series evaluation of surgical status using AI object recognition model in colorectal surgery

Yoshiko BAMBA, Shimpei OGAWA, Yuka KANEKO, Ryo Futatsuki, Kurodo KOSHINO, Kimitaka TANI, Fumi MAEDA, Yurin KONDO, Shigeki YAMAGUCHI

Department of Surgery, Institute of Gastroenterology, Tokyo Women's Medical University, Tokyo JAPAN

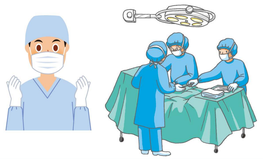
Total Navigation Surgery(TNS)

Total Navigation Surgery is an advanced surgical approach that integrates cutting-edge AI technologies, real-time data analysis, and precision guidance systems to enhance surgical accuracy, safety, and efficiency. By leveraging AI-driven insights, this concept enables surgeons to make more informed decisions during procedures, reducing complications and improving patient outcomes.

Preoperative AI Imaging Diagnosis



AI Navigation Surgery



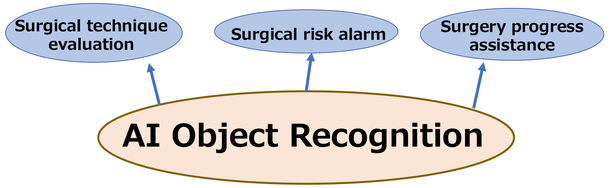
Perioperative AI Risk Management



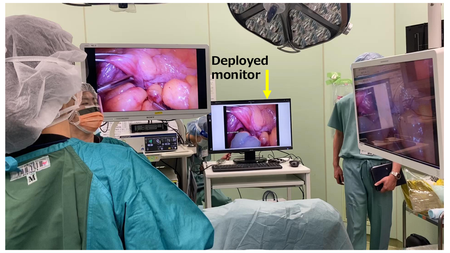
AI Navigation Surgery

Optimal surgery for patients who avoid risks by analyzing preoperative images and intraoperative procedures using artificial AI and returning useful information to the surgeon during surgery

AI navigation surgery require AI Object Recognition a basis for decision-making.



Real−time AI Object Recognition



May 2022

A workstation is installed next to the laparoscopic surgery monitor, allowing real-time results to be obtained almost simultaneously

AI object recognition model

This study presents an AI object recognition model tailored for colorectal cancer surgery. Using 11,225 annotated images derived from 57 surgical videos, the model was trained to recognize 26 types of objects, including surgical instruments (e.g., forceps, staplers) and anatomical structures (e.g., vessels, gastrointestinal tract).

Object	Average precision	Recall	IoU
Grasping F 5082 objects / 3809 images	0.819	0.999	0.523
Harmonic F 2173 objects / 2166 images	0.894	1	0.707
Angled F 1223 objects / 1223 images	0.945	1	0.734
Clip F 1103 objects / 1094 images	0.982	1	0.703
Suction F 1068 objects / 1068 images	0.931	1	0.569
Needle holder 173 objects / 148 images	0.873	1	0.554
Linear S 930 objects / 930 images	0.982	1	0.604
Circular S 596 objects / 596 images	0.973	1	0.61
Anvil 667 objects / 665 images	0.993	1	0.544
Clip 3849 objects / 1826 images	0.879	0.976	0.454
Big clip 1307 objects / 1306 images	0.907	0.996	0.474
Gauze 2545 objects / 1775 images	0.81	0.994	0.502
Tape 223 objects / 174 images	0.695	0.969	0.381
Drain tube 167 objects / 159 images	0.858	0.974	0.501
Needle 123 objects / 123 images	0.494	0.933	0.382

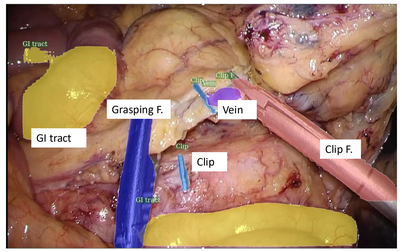
Object	Average precision	Recall	IoU
GI tract 2934 objects / 1994 images	0.698	0.982	0.397
Liver 777 objects / 697 images	0.907	1	0.48
GB 352 objects / 352 images	0.934	1	0.554
Uterus 410 objects / 410 images	0.849	0.987	0.564
Ovary 424 objects / 376 images	0.941	1	0.575
Ureter 433 objects / 429 images	0.774	0.958	0.402
Artery 1283 objects / 1225 images	0.8	0.957	0.374
Vein 1314 objects / 1071 images	0.815	0.947	0.411
Blood 2053 objects / 1200 images	0.637	0.933	0.344
Bleeding 941 objects / 576 images	0.814	0.983	0.352
Airy layer 1122 objects / 893 images	0.786	0.944	0.35
BV stump 1089 objects / 788 images	0.903	0.99	0.513
Rectal stump 412 objects / 407 images	0.815	0.989	0.51
Nerve 165 objects / 130 images	0.244	0.583	0.371

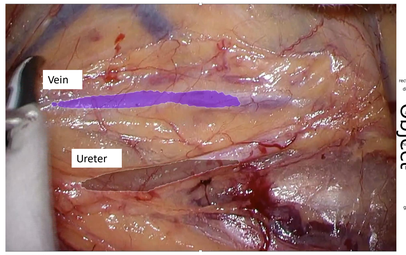
Diagnostic test result of object detection model

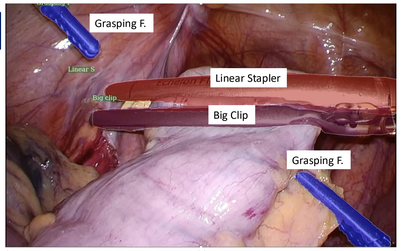
Evaluation on 600 still images from seven laparoscopic surgical videos yielded promising results, with an average recall of 85.2% and precision of 90.8%.

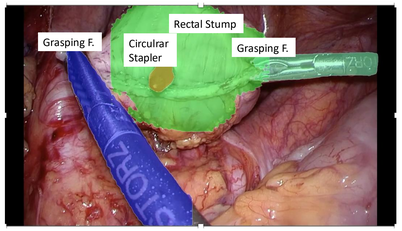
	Number of object in images	Number of object pointed out correctly	Number of object not pointed out	False positive	Sensitivity	Positive predictive value (PPV)
Grasping F	618	532	86	57	86.1% (532/618)	90.3% (532/589)
Harmonic F	145	140	5	10	96.6% (140/145)	93.3% (140/150)
Angled F	66	62	4	13	93.9% (62/66)	82.7% (62/75)
Clip F	45	45	0	6	100% (45/45)	88.2% (45/51)
Suction F	43	40	3	27	93.0% (40/43)	59.7% (40/67)
GI tract	438	300	138	3	68.5% (300/438)	99.0% (300/303)
Artery	104	98	6	25	94.2% (98/104)	79.7% (98/123)
Vein	53	49	4	6	92.5% (49/53)	89.1% (49/55)
Blood	246	215	31	0	87.4% (215/246)	100% (215/215)
Bleeding	86	76	10	3	88.4% (76/86)	96.2% (76/79)
BV Stump	75	59	16	4	78.7% (59/75)	93.7% (59/63)
Airy Layer	56	56	0	2	100% (56/56)	96.6% (56/58)
Gauze	124	109	15	6	87.9% (109/124)	94.8% (109/115)
Clip	197	171	23	9	86.8% (171/197)	95.0% (171/180)
Uterus	38	32	6	0	81.6% (31/38)	100% (32/32)
Ovary	21	14	7	3	66.7% (14/21)	82.4% (14/17)
Ureter	19	16	3	7	84.2% (16/19)	69.6% (16/23)
Liver	45	40	5	12	88.9% (40/45)	76.9% (40/52)
GB	23	19	4	3	82.6% (19/23)	86.4% (19/22)
Rectal Stump	54	50	4	3	82.6% (50/54)	100% (50/53)
Big Clip	88	77	11	26	92.3% (24/26)	82.8% (24/29)
Linear S	36	31	5	3	86.1% (31/36)	91.2% (31/34)
Anvil	41	39	2	5	95.1% (39/41)	88.6% (39/44)
Circular S	39	37	2	1	94.9% (37/39)	97.4% (37/38)
Tape	25	21	4	2	84.0% (21/25)	91.3% (21/23)
Drain Tube	42	33	9	7	78.6% (33/42)	82.5% (33/40)

Inference Results by AI object recognition model



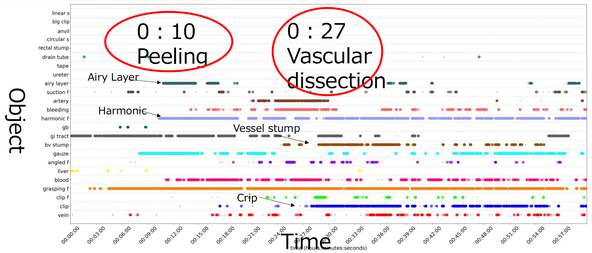


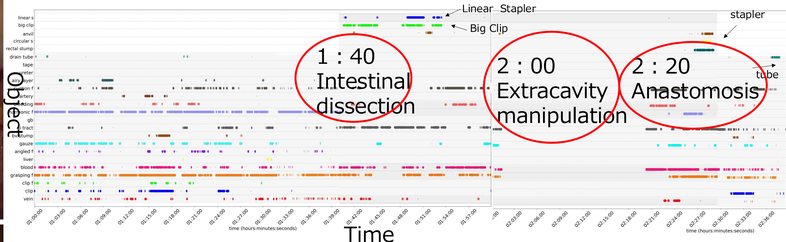




Time-series evaluation of surgical status using AI object recognition model

Operation : Laparoscopic Sigmoid Resection 2hr 40min

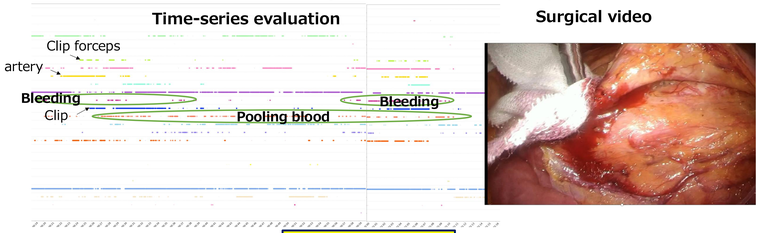




Temporal evaluation of surgical workflows identified critical events such as dissection initiation, vascular handling, and anastomosis, correlating well with actual procedural timelines. These findings confirm the feasibility of using object recognition models for real-time and time-series assessment of surgical progress.

Detection of bleeding scenes

Bleeding scene detection is possible through time-series evaluation.



Conclusion

This foundational research demonstrates the potential of integrating AI into surgical workflows, paving the way for next-generation systems that can optimize operations, support skill transfer, and address critical challenges in surgery.